

Spin tune in the single resonance model with a pair of Siberian Snakes ¹

D. P. Barber^{*}, R. Jaganathan[†] and M. Vogt^{*}

^{*}*Deutsches Elektronen-Synchrotron, DESY, 22603 Hamburg, Germany.*

[†]*The Institute of Mathematical Sciences, Chennai. Tamilnadu 600113, India.*

Abstract. Snake “resonances” are classified in terms of the invariant spin field and the amplitude dependent spin tune. Exactly at snake “resonance” there is no continuous invariant spin field at most orbital amplitudes.

PROLOGUE

This is an extended version of the paper with the same title published in the proceedings of the conference SPIN2002 [1]. A key aspect of the original paper was that the invariant spin field for snake “resonances” is irreducibly discontinuous at most orbital amplitudes. However, details were omitted owing to the page limit. In the meantime other papers [2, 3] have appeared which discuss the invariant spin field at snake “resonances” and it has become clear that it would be useful to extend [1] to give more details.

We begin by presenting a slightly polished version of the original paper. Then the additional material is presented as an addendum. The citations are also updated.

INTRODUCTION

Spin motion in storage rings and circular accelerators is most elegantly systematised in terms of the invariant spin field (ISF) and the amplitude dependent spin tune (ADST). Here we apply them in the context of snake “resonances”. We begin by briefly recapitulating some necessary basic ideas. For more details see [4, 5, 6, 7].

Spin motion in electric and magnetic fields at the 6-dimensional phase space point \vec{z} and position s around the ring, is described by the T-BMT precession equation $d\vec{S}/ds = \vec{\Omega}(\vec{z}; s) \times \vec{S}$ [8, 4] where \vec{S} is the spin expectation value (“the spin”) in the rest frame of the particle and $\vec{\Omega}(\vec{z}; s)$ contains the electric and magnetic fields in the laboratory. The ISF, denoted by $\hat{n}(\vec{z}; s)$, is a 3-vector *field* of unit length obeying the T-BMT equation along particle orbits $(\vec{z}(s); s)$ and fulfilling the periodicity condition $\hat{n}(\vec{z}; s + C) = \hat{n}(\vec{z}; s)$ where C is the circumference. Thus $\hat{n}(\vec{M}(\vec{z}; s); s + C) = \hat{n}(\vec{M}(\vec{z}; s); s) = R_{3 \times 3}(\vec{z}; s) \hat{n}(\vec{z}; s)$ where $\vec{M}(\vec{z}; s)$ is the new phase space vector after one turn starting at \vec{z} and s and $R_{3 \times 3}(\vec{z}; s)$

¹ DESY Report: DESY 05-035 and physics/0502121

is the corresponding spin transfer matrix. The scalar product $J_s = \vec{S} \cdot \hat{n}$ is invariant along an orbit, since both vectors obey the T-BMT equation. Thus with respect to the local \hat{n} the motion of \vec{S} is simply a precession around \hat{n} . The field \hat{n} can be constructed at each reference energy where it exists without reference to individual spins.

The chief aspects of the ISF are that: 1) For a turn-to-turn invariant particle distribution in phase space, a distribution of spins initially aligned along the ISF remains invariant (in equilibrium) from turn-to-turn, 2) for integrable orbital motion and away from orbital resonances and spin-orbit resonances (see below), the ISF determines the maximum attainable time averaged polarisation $P_{\text{lim}} = |\langle \hat{n}(\vec{z}; s) \rangle|$ on a phase space torus at each s , where $\langle \rangle$ denotes the average over the orbital phases, 3) under appropriate conditions J_s is an adiabatic invariant while system parameters such as the reference energy are slowly varied, 4) it provides the main axis for orthonormal coordinate systems at each point in phase space which serve to define the ADST which in turn is used to define the concept of spin-orbit resonance.

These coordinate systems are constructed by attaching two other unit vectors $\hat{u}_1(\vec{z}; s)$ and $\hat{u}_2(\vec{z}; s)$ to all (\vec{z}, s) such that the sets $(\hat{u}_1, \hat{u}_2, \hat{n})$ are orthonormal. Like \hat{n} , the *fields* \hat{u}_1 and \hat{u}_2 are 1-turn periodic in s : $\hat{u}_i(\vec{z}; s + C) = \hat{u}_i(\vec{z}; s)$ for $i \in \{1, 2\}$. With the basis vectors \hat{u}_1 and \hat{u}_2 we can quantify the rate of the above mentioned spin precession around \hat{n} : it is the rate of rotation of the projection of \vec{S} onto the \hat{u}_1, \hat{u}_2 plane. Except on or close to orbital resonance, the fields $\hat{u}_1(\vec{z}; s)$ and $\hat{u}_2(\vec{z}; s)$ can be chosen so that the rate of precession is constant and independent of the orbital phases [9, 5, 6, 7]. The number of precessions per turn “measured” in this way is called the spin tune. The spin tune, $\nu_s(\vec{J})$, depends only on the orbital amplitudes (actions) \vec{J} , hence the name ADST. The choice of some $\hat{u}_1(\vec{z}; s)$ and $\hat{u}_2(\vec{z}; s)$ satisfying the condition $\hat{u}_i(\vec{z}; s + C) = \hat{u}_i(\vec{z}; s)$ for $i \in \{1, 2\}$ is not unique. An infinity of others can be chosen by suitable rotations of the \hat{u}_i around \hat{n} . These lead to the *equivalence class* of spin tunes obtained by the transformation: $\nu_s(\vec{J}) \Rightarrow \nu_s(\vec{J}) + l_0 + l_1 Q_1 + l_2 Q_2 + l_3 Q_3$ for any integers l where the $Q(\vec{J})$'s are the tunes on a torus of integrable orbital motion ². The ADST provides a way to quantify the degree of coherence between the spin and orbital motion and thereby predict how strongly the electric and magnetic fields along particle orbits disturb spins. In particular, the spin motion can become very erratic close to the *spin-orbit resonance* condition $\nu_s(\vec{J}) = m_0 + m_1 Q_1 + m_2 Q_2 + m_3 Q_3$ where the m 's are integers. At these resonances the ISF can spread out so that P_{lim} is very small. Examples of the behaviour of P_{lim} near spin-orbit resonance and the application of a generalised Froissart-Stora description of the breaking of the adiabatic invariance of J_s while crossing resonances during variation of system parameters can be found in [6, 7, 10, 11]. Note that: 1) the resonance condition is *not* expressed in terms of the spin tune $\nu(\vec{0})$ on the closed orbit, 2) a “tune” describing spin motion but depending on orbital phases could not be meaningful in the spin-orbit resonance condition, 3) if the system is on spin-orbit resonance for one spin tune of the equivalence class, it is on resonance for all others. In general \hat{u}_1 and \hat{u}_2 do not obey the T-BMT equation along an orbit $(\vec{z}(s); s)$. But at spin-orbit resonance, they can be chosen so that a spin \vec{S} is at rest in its local $(\hat{u}_1, \hat{u}_2, \hat{n})$ system. Then $\hat{u}_1(\vec{z}; s)$ and $\hat{u}_2(\vec{z}; s)$

² For a recent detailed discussion of these concepts, see [3].

do obey the T–BMT equation so that the ISF $\hat{n}(\vec{z}; s)$ is not unique.

Nowadays we emphasise the utility of the ISF for defining equilibrium spin distributions. However, it was originally introduced for bringing the combined semiclassical Hamiltonian of spin–orbit motion into action–angle form for calculating the effects of synchrotron radiation [12]. The initial Hamiltonian is written as $H_{s-o} = \frac{2\pi}{C}(Q_1J_1 + Q_2J_2 + Q_3J_3) + \vec{\Omega} \cdot \vec{S}$. By viewing the spin motion in the $(\hat{u}_1, \hat{u}_2, \hat{n})$ systems, a new Hamiltonian in full action–angle form $H_{s-o}^{aa} = \frac{2\pi}{C}(Q'_1J'_1 + Q'_2J'_2 + Q'_3J'_3) + \frac{2\pi}{C}v_s(\vec{J})J_s$ is obtained which is valid at first order in \hbar [9]. This emphasises again that, as with all action–angle formulations, the spin frequency cannot depend on orbital phases. Moreover, it is easy to show that at orbital resonance, (i.e. $k_0 + k_1Q_1 + k_2Q_2 + k_3Q_3 = 0$ for suitable integers k) the “diagonalisation” of the Hamiltonian (i.e. finding the \hat{u}_1, \hat{u}_2) might not be possible [9, 3]. Thus at orbital resonance the ADST may not exist. On the other hand, one avoids running a machine on such resonances. The spin tune on the closed orbit $\nu_0 = \nu_s(\vec{0})$ always exists and so does $\hat{n}_0(s) = \hat{n}(\vec{0}; s)$. The terms at first order in \hbar describe forces of the Stern–Gerlach type. However, these are extremely small and as explained in detail in [3] the Lorentz force and T–BMT precession are then perfectly adequate for studying spin motion in real storage rings. A formulation in terms of a spin–orbit Hamiltonian has no obvious conceptual or practical advantage if only the effects of external electric and magnetic fields are to be considered.

For our present purposes there are two kinds of orbital resonances: resonances where at least one of the Q ’s is irrational and those where all are rational. We write the rational tunes as $Q_i = a_i/b_i$ ($i = 1, 2, 3$) where the a_i and b_i are integers. Then for the second type, the orbit is periodic over c turns where c is the lowest common multiple of the b_i . This opens the possibility that in this case the ISF at each (\vec{z}, s) can be obtained (up to a sign) as the unit length real eigenvector of the c –turn spin map (c.f. the calculation of \hat{n}_0 from the 1–turn spin map on the closed orbit.). However, the corresponding eigentune $c\nu_c$ extracted from the complex eigenvalues $\lambda_c = e^{\pm 2\pi i c \nu_c}$, depends in general on the orbital phases at the starting \vec{z} . Thus in general ν_c is *not* a spin tune and should not be so named [13]. Nevertheless if c is very large the dependence of ν_c on the phases can be very weak so that it can approximate well the ADST of nearby irrational tunes. This is expected heuristically since the influence of the starting phase can be diluted on forming the spin map for a large number of turns. At non–zero amplitudes, both for irrational or rational Q ’s, the eigentune of the 1–turn spin map usually has no physical significance. Of course, it normally depends on the orbital phases and the corresponding eigenvectors are normally not even solutions of the T–BMT equation.

For non–resonant orbital tunes, the spin tune can be obtained using the SODOM–II algorithm [14] whereby spin motion is written in terms of two component spinors and SU(2) spin transfer matrices. The *functional equation* $\hat{n}(\vec{M}(\vec{z}; s); s) = R_{3 \times 3}(\vec{z}; s)\hat{n}(\vec{z}; s)$ is then expressed in terms of a Fourier representation, w.r.t. the orbital phases, of the spinors and of the 1–turn SU(2) matrices. The spin tune appears as the set of eigentunes of an *eigen problem for Fourier components* and \hat{n} is reconstructed from the Fourier eigenvectors. SODOM–II delivers the whole spin field on the torus \vec{J} at the chosen s .

THE SINGLE RESONANCE MODEL

In perfectly aligned flat rings with no solenoids, \hat{n}_0 is vertical and v_0 is in the equivalence class containing $a\gamma_0$ where γ_0 is the Lorentz factor on the closed orbit and a is the gyromagnetic anomaly of the particle. In the absence of skew quadrupoles, the primary disturbance to spin is then from the radial magnetic fields along vertical betatron trajectories. The disturbance can be very strong and the polarisation can fall if the particles are accelerated through the condition $a\gamma_0 = \kappa \equiv k_0 \pm Q_2$ where mode 2 is vertical motion. This can be understood in terms of the “single resonance model” (SRM) whereby a rotating wave approximation is made in which the contribution to $\vec{\Omega}$ from the radial fields along the orbit is dominated by the Fourier harmonic at κ with strength $\varepsilon(J_2)$. The SRM can be solved exactly and the ISF is given by [15] $\hat{n}(\phi_2) = \text{sgn}(\delta) (\delta \hat{e}_2 + \varepsilon(\hat{e}_1 \cos \phi_2 + \hat{e}_3 \sin \phi_2)) / \sqrt{\delta^2 + \varepsilon^2}$ where $\delta = a\gamma_0 - \kappa$, ϕ_2 is the orbital phase, $(\hat{e}_1, \hat{e}_2, \hat{e}_3)$ are horizontal, vertical and longitudinal unit vectors and the convention $\hat{n} \cdot \hat{e}_2 \geq 0$ is used. The tilt of \hat{n} away from the vertical \hat{n}_0 is $|\arcsin(\varepsilon/\sqrt{\delta^2 + \varepsilon^2})|$ so that it is 90° at $\delta = 0$ for non-zero ε . At large $|\delta|$, the equilibrium polarisation directions $\hat{n}(J_2, \phi_2; s)$, are almost parallel to $\hat{n}_0(s)$ but during acceleration through $\delta = 0$, \hat{n} varies strongly and the polarisation will change if the adiabatic invariance of J_s is violated. The change in J_s for acceleration through $\delta = 0$ is given by the Froissart–Stora formula. The ADST which reduces to $a\gamma_0$ on the closed orbit is $v_s = \text{sgn}(\delta) \sqrt{\delta^2 + \varepsilon^2} + \kappa$. Note that the condition $\delta = 0$ is *not* the spin–orbit resonance condition. On the contrary, as δ passes through zero v_s jumps by 2ε with our convention for \hat{n} and avoids fulfilling the true resonance condition: for particles with non-zero ε , $a\gamma_0$ is just a parameter. In this simple model v_s exists and is well defined near spin–orbit resonances for all Q_2 . This is also true in more general cases if orbital resonance is avoided.

THE SINGLE RESONANCE MODEL WITH A PAIR OF SIBERIAN SNAKES

Snake “resonances”

Polarisation loss while accelerating through $\delta = 0$ can be reduced by installing pairs of Siberian Snakes, magnet systems which rotate spins by π independently of \vec{z} around a “snake axis” in the machine plane. For example, one puts two snakes at diametrically opposite points on the ring. Then $\hat{n}_0 \cdot \hat{e}_2 = +1$ in one half ring and -1 in the other. With the snake axes relatively at 90° , v_0 is in the equivalence class containing $1/2$ for all γ_0 . For calculations one often represents the snakes as elements of zero length (“pointlike snakes”). Then if, in addition, the effect of vertical betatron motion is described by the SRM, and orbital resonances are avoided, calculations with SODOM–II, perturbation theory [16] and the treatment in [13] suggest that $v_s(J_2)$ is in the equivalence class containing $1/2$ too, independently of γ_0 but also of J_2 . Thus for Q_2 sufficiently away from $1/2$ no spin–orbit resonances $v_s(J_2) = k_0 \pm Q_2$ are crossed during acceleration through $\delta = 0$ and the polarisation can be preserved. This is confirmed by tracking

calculations. However, such calculations and analytical work show that the polarisation can still be lost if the fractional part of Q_2 , $[Q_2]$, is $\tilde{a}_2/2\tilde{b}_2$ where here, and later, \tilde{a}_2 and \tilde{b}_2 are odd positive integers with $\tilde{a}_2 < 2\tilde{b}_2$ and where here and later the brackets [...] are used to signal the fractional part of a number. This is the so-called “snake resonance phenomenon” and it also has practical consequences [17, 18, 19], especially for small \tilde{b}_2 . Such a $[Q_2]$ fits the condition $1/2 = (1 - \tilde{a}_2)/2 + \tilde{b}_2[Q_2]$. But calculations (see below) show that exactly at $[Q_2] = \tilde{a}_2/2\tilde{b}_2$ the ADST may not exist. If it doesn’t, it isn’t in the equivalence class for $1/2$. Then we are not dealing with a conventional resonance $v_s(J_2) = (1 - \tilde{a}_2)/2 + \tilde{b}_2[Q_2]$ and the term *resonance* is inappropriate. Depolarisation in this model has also been attributed to the fact that for non-zero J_2 the eigentune of the 1–turn spin map, which depends on ϕ_2 , is $1/2$ at some values of ϕ_2 [17]. However, such a quantity does not describe spin–orbit coherence. Snake “resonances” are usually associated with acceleration but it has been helpful in other circumstances [6, 7, 10] to begin by studying the *static* properties of the system, namely with the ISF. We now do that for the SRM with two snakes for representative, parameters.

Numerical study

Figure 1 shows P_{lim} (just before a snake) and v_s for 25000 equally spaced $[Q_2]$ ’s between 0 and 0.5 for $\varepsilon = 0.4$ and $\delta = 0$. At each $[Q_2]$, \hat{n} is calculated by stroboscopic averaging [4] ($\leq 25 \cdot 10^6$ turns) at 500 equally spaced ϕ_2 in the range $0 - 2\pi$ and P_{lim} is obtained by averaging over these ϕ_2 . The ADST is obtained from SODOM–II. If the ADST exists SODOM–II delivers a part of the equivalence class, namely the spectrum $[\pm 0.5 + l_2 Q_2]$ for a range of contiguous even l_2 restricted by the necessarily finite size of the matrix of Fourier coefficients. Only even l_2 are allowed by the algorithm. For irrational Q_2 the range of l_2 is large. For rational Q_2 the spectrum can include ± 0.5 but is otherwise highly degenerate or contains none or just a very few of the required members $[\pm 0.5 + l_2 Q_2]$. Thus the existence of an ADST is easily checked. The central horizontal row of points in figure 1 shows the common member $+0.5$ of the equivalence class of the ADST at the values of $[Q_2]$ where the ADST exists. There is an ADST for most $[Q_2]$ ’s used. The first row of dots up from the bottom marks $[Q_2]$ values where there is no ADST. As expected, these are all at rational $[Q_2]$ ’s such as $1/5, 1/4, 2/5 \dots$ or $\tilde{a}_2/2\tilde{b}_2 = 1/6, 3/14, 3/10 \dots$ and the $[cvc]$ computed for these $[Q_2]$ show ϕ_2 dependence. The curved line shows P_{lim} and the second row of dots from the bottom marks $[Q_2]$ values where the ISF obtained by stroboscopic averaging did not converge for all phases. These coincide with sharp dips in P_{lim} and are at or near $[Q_2] = \tilde{a}_2/2\tilde{b}_2$, i.e in the snake “resonance” subset of the $[Q_2]$ ’s in the first row. Thus snake “resonance” is already a static phenomenon. Near such $[Q_2]$ ’s, the ISF, which for just one orbital mode is a closed curve in three dimensions, becomes extremely complicated as \hat{n} strives to satisfy its defining conditions. Right at $[Q_2] = \tilde{a}_2/2\tilde{b}_2$ the nonconvergence occurs at $[\phi_2/2\pi] = j/2\tilde{b}_2$ for integers $j = 1, \dots, 2\tilde{b}_2$ and, moreover, *the ISF is discontinuous*

at these phases³. For $[Q_2] = \tilde{a}_2/4\tilde{b}_2$ ($\tilde{a}_2 < 4\tilde{b}_2$), P_{lim} and the ISF show no special behaviour. These observations are consistent with the perturbative result [7] that for mid-plane symmetric systems, \hat{n} should be well behaved near even m_2 but may show exotic behaviour close to odd $m_2 = \tilde{b}_2$. As expected, P_{lim} and the ISF also show no special behaviour for $[Q_2] = a_2/\tilde{b}_2$ ($a_2 < \tilde{b}_2$). Some snake “resonances” such as that at $[Q_2] = 1/30$ are narrower than 0.00002 in $[Q_2]$ and are missed in this scan. P_{lim} also has several dips at values of $[Q_2]$ (e.g. at 0.341) which appear to have no special significance, but which should still be avoided at storage. The results for $0.5 \leq [Q_2] \leq 1.0$ are the reflection in 0.5 of the curves and points shown. Qualitatively similar results are obtained with equally distributed odd pairs of snakes set to give $\nu_0 = 1/2$. The ISF and P_{lim} usually vary significantly with s .

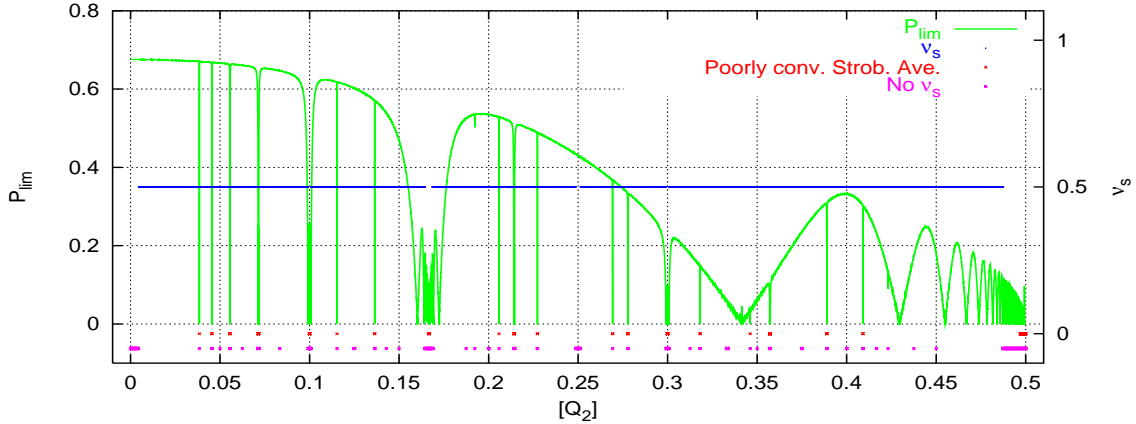


FIGURE 1. P_{lim} (left axis) and a component of the ADST (right axis) for the SRM with $\delta = 0$, $\varepsilon = 0.4$ and with 2 Siberian Snakes with axes at 90° and 0° .

Addendum

A typical example for an ISF at a snake “resonance” is shown in figure 2. This shows the components of the ISF for $[Q_2] = 1/6$ and $\varepsilon = 0.4$. In this case they are obtained by using the 6–turn spin map to calculate the vector \hat{n} in the range $0 < [\phi_2/2\pi] \leq 1/2\tilde{b}_2$, namely 0 to 60 degrees, while applying the constraint that \hat{n} should be continuous in ϕ_2 . Then the \hat{n} for each ϕ_2 in this range is transported with the 1–turn spin map for six, or more, turns. One sees that \hat{n} changes sign at values of ϕ_2 which are multiples of 60 degrees so that the ISF is discontinuous as advertised. The six sets of stray points at $[\phi_2/2\pi] = 1/12, 1/4 \dots$ are at phases ϕ_2 where the 6–turn spin map is the identity. At these phases \hat{n} obtained in this way is arbitrary and the algorithm delivers values dominated by numerical noise. Of course, if the ISF is represented as the locus of points on the surface of the unit 2–sphere, this ISF gives disjoint segments. The positions of the

³ Note that in [3] it was convenient to require that the magnetic and electric fields and the ISF were smooth in ϕ and s . Here we drop that requirement since we are dealing with models with pointlike snakes.

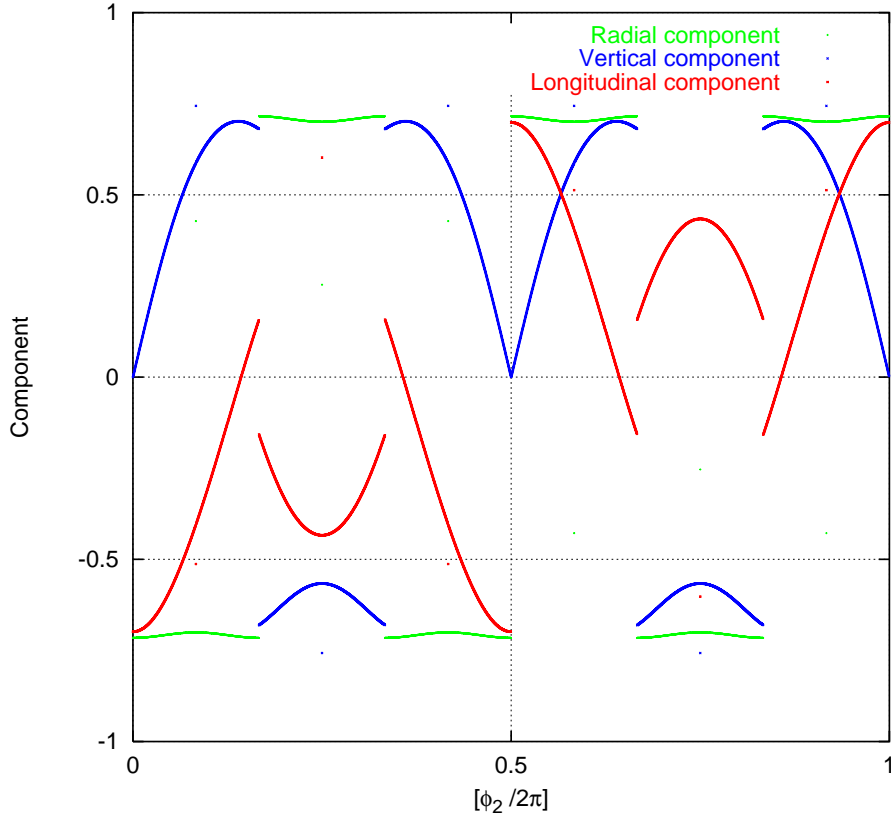


FIGURE 2. The three components of $\hat{n}(\phi_2)$ for the SRM with 2 Siberian Snakes with axes at 90° and 0° and for $[Q_2] = 1/6$. Viewing point: just before a snake. $\delta = 0$ and $\varepsilon = 0.4$.

discontinuities can be shifted by changing the sign of \hat{n} at some phase in the range 0 to 60° degrees. Furthermore extra discontinuities can be added by hand in the same way. Thus at snake “resonances” the invariant spin field is not only discontinuous but also *non-unique* and to an extent which goes far beyond the non-uniqueness at the phases ϕ_2 at which the 6–turn spin map is the identity. The ISF shows analogous behaviour at other snake “resonances”. The “fragmentation” of the ISF at snake “resonances” is in stark contrast to the case, say, of the pure SRM where the ISF varies smoothly with ϕ_2 at all values of the system parameters. Note that an ISF with continuous segments separated by discontinuities would not be allowed for irrational $[Q_2]$, but that such an ISF is not prohibited for rational $[Q_2]$. Moreover, it can be shown that the uniqueness of the ISF is only guaranteed if the system is away from orbital resonance and if a spin tune exists [3, 6, 7]. Of course, for snake “resonances” with very high values of \tilde{b}_2 , the ISF and the corresponding configuration of equilibrium polarisation is very complicated. It is then far from clear whether the ISF is a useful concept for these simple models involving just one plane of orbital motion and singular, i.e., non-physical fields, although, of course, such models have been instrumental in presaging the loss of polarisation observed in real storage rings [17, 18, 19].

The ISF obtained from the real eigenvector of the multi–turn spin map is also non–unique for $[Q_2] = \tilde{a}_2/4\tilde{b}_2$, namely at those $[\phi_2/2\pi]$ where the $4\tilde{b}_2$ –turn spin map is the identity. Moreover, additional discontinuities in the sign can be added by hand, thereby enhancing the choice of ISF’s. But in contrast to the case of snake “resonances” such discontinuities remain optional. Analogous considerations apply when $[Q_2] = \tilde{a}_2/\tilde{b}_2$ or $[Q_2] = 2\tilde{a}_2/\tilde{b}_2$.

Further aspects of these matters will be reported elsewhere.

It is instructive to compare the discontinuous curves in figure 2 with the smooth curves in figures 7 and 8 in [2]⁴. These are also said to represent ISF’s at snake “resonances”. The vectors corresponding to the curves in figure 2 satisfy the T–BMT equation by construction and they are single valued in $[\phi_2/2\pi]$ as required for an ISF. However, if the vectors for the curves in figures 7 and 8 in [2] are transported according to the T–BMT equation, they are not single valued in $[\phi_2/2\pi]$. Alternatively, if those curves are taken to represent single–valued functions of $[\phi_2/2\pi]$, as depicted, then they do not represent spin motion, i.e., motion according to the T–BMT equation. Either way, the curves in those figures do not represent ISF’s at snake “resonances”.

SUMMARY

A snake “resonance” is at root a *static* phenomenon characterised by an invariant spin field which, for the simple models discussed here, is irreducibly discontinuous in ϕ_2 for most orbital amplitudes. Moreover, on and near snake “resonance”, there is no amplitude dependent spin tune so that the snake “resonances” of these models are not simple spin–orbit resonances. The mechanism, in terms of J_s , for polarisation loss during acceleration through $\delta = 0$ at and near such $[Q_2]$ ’s is under study.

We thank K. Heinemann, G. H. Hoffstaetter and J.A. Ellison for useful discussions.

REFERENCES

1. D.P. Barber, R. Jaganathan and M. Vogt, Proc. 15th Int. Spin Physics Symposium, Brookhaven National Laboratory, Long Island, U.S.A., September 2002. AIP proceedings 675 (2003).
2. S.R. Mane, Nucl. Instr. Meth. **A528** 667 (2004).
3. D.P.Barber, J.A. Ellison and K. Heinemann, Phys. Rev. ST Accel. Beams **7**(12), 124002 (2004).
4. K. Heinemann and G.H. Hoffstaetter, Phys.Rev. **E 54**(4) 4240 (1996).
5. G.H. Hoffstaetter, M. Vogt and D.P. Barber, Phys. Rev. ST Accel. Beams **11**(2) 114001 (1999).
6. G.H. Hoffstaetter, “*A modern view of high energy polarised proton beams*”, To be published as a Springer Tract in Modern Physics.
7. M. Vogt, Ph.D. Thesis, University of Hamburg, DESY-THESIS-2000-054 (2000).
8. J.D. Jackson, “*Classical Electrodynamics*”, 3rd edition, Wiley (1998).
9. K. Yokoya, DESY report 86-57 (1986).
10. D.P. Barber, G.H. Hoffstaetter and M. Vogt, SPIN 2000, AIP proceedings 570 (2001).

⁴ It is also shown in [2] that the curve in figure 1 can be reproduced by the MILES algorithm by the same author. MILES, like SODOM–II, is based on SU(2) and Fourier expansions.

11. G.H. Hoffstaetter and M. Vogt, Phys. Rev. E **70**, 056501 (2004).
12. D.P. Barber et al., in “*Quantum Aspects of Beam Physics*”, Monterey, 1998, World Scientific (1999).
13. S.R. Mane, Nucl. Instr. Meth. **A480**, p.328 and **A485**, p.277 (2002).
14. K. Yokoya, DESY report 99-006 (1999), Los Alamos archive: physics/9902068.
15. S.R. Mane, Fermilab technical report TM-1515 (1988).
16. K. Yokoya, SSC CDG report SSC-189 (1988).
17. S.Y. Lee, “*Spin Dynamics and Snakes in Synchrotrons*”, World Scientific (1997).
18. A.Luccio, V.Ptitsyn and V. Ranjbar, Proc. 15th Int. Spin Physics Symposium, Brookhaven National Laboratory, Long Island, U.S.A., September 2002. AIP proceedings 675 (2003).
19. M. Bai et al., Proc. 16th Int. Spin Physics Symposium, Trieste, Italy, October (2004). To be published by World Scientific.